Aeroacoustics Conferences
June 4-7, 2024, Rome, Italy
30th AIAA/CEAS Aeroacoustics Conference (2024)

10.2514/6.2024-3159

Noise reduction of aero-engines using innovative stators with leading edge features

Édouard Salze*, Antonio Pereira, Christoph Brandstetter and Vincent Clair
Univ Lyon, CNRS, Ecole Centrale de Lyon, INSA Lyon, Univ Claude Bernard Lyon 1, LMFA, UMR5509, 69131 Écully, France

Fernando Gea-Aguilera, David Lamidel and Jacky Mardjono
Safran Aircraft Engines, Département Aérodynamique et Acoustique, 77550 Moissy Cramayel, France

Martin Buszyk and Cyril Polacsek
ONERA, DAAA, Université Paris-Saclay, 92320 Châtillon, France

Raluca Maier, Cristian Stanica, Valeriu Dragan and Teodor Stanescu
Composite Materials Laboratory for Aeronautical Field, Romanian Research & Development Institute for Gas Turbines — COMOTI, 061126 Bucharest, Romania

Michael Bauer†
Munich Aeroacoustics UG, 85551 Kirchheim b. München, Germany

This work is dedicated to the aeroacoustic characterization of low-noise outlet guide vanes with leading edge features, designed for the reduction of UHBR turbofan noise in the framework of European Project Cleansky 2 H2020 INNOSTAT. Two innovative low-noise OGV concepts with leading edge serrations and slits were designed, fabricated, and tested on the ECL5 - CATANA fan stage, which is used as reference for the aeroacoustic performance of a realistic turbofan test-case. Detailed aerodynamic and acoustic measurements were performed for different operating conditions of the fan stage. The instrumentation includes rakes, a far-field microphone array, and flush-mounted microphones to analyze the modal content of the fan-OGV noise. Both low-noise OGV concepts show promising results from an aeroacoustic perspective. Broadband noise can be reduced up to 4 dB for the slitted OGV and up to 6 dB for the serrated OGV in upstream direction. Downstream of the fan-OGV stage, the in-duct modal decomposition shows a broadband noise reduction of approximately 8 dB for the high-order modes, which leads to a reduction in the acoustic power of 5 to 10 dB for both concepts over a large portion of the frequency range. Additionally, a significant attenuation of the blade passing frequency harmonics can be observed in the upstream and downstream directions (up to 13 dB for the slitted OGV). These findings suggest that innovative leading edge features on the OGVs can be useful to reduce broadband and tonal interaction noise in modern aero-engines.

Keywords: aeroacoustics, fan-OGV noise, low-noise stator, leading edge features, serrations, slits

I. Introduction

The next generation of aero-engines presents an ultra high by-pass ratio (UHBR), which is suitable to reduce fuel consumption. However, UHBR aero-engines present several challenges in terms of noise emissions that need to be addressed. For example, UHBR turbofan engines may have a short and thin nacelle, and present a noise spectrum dominated by low frequencies. This is due to the reduced rotational speed and the increased fan diameter. Noise reduction that can be achieved using conventional acoustic liners may be reduced, as less surface will be available within a short and thin nacelle. In order to overcome these challenges, innovative noise reduction technologies could be required for the next generation of commercial aero-engines.

*corresponding author, edouard.salze@ec-lyon.fr
†AIAA Senior Member

The main noise source of UHBR turbofan engines is due to the interaction between the fan wakes and the outlet guide vanes (OGV), which produces both tonal and broadband noise from the OGV leading edge. This paper focuses on passive noise reduction, achieved through unconventional low-noise outlet guide vanes (OGVs). It is well known that the interaction noise can be reduced using leading edge features on isolated airfoils[1, 14], rectilinear cascades[5] and OGVs[8, 17], as it is useful to decorrelate noise sources along the span.

This paper presents experimental results of the collaborative European H2020 CleanSky 2 Project INNOSTAT [11], in which several low-noise OGV concepts were designed and tested to increase their technology readiness level (TRL). Firstly, a rectilinear cascade was built and tested in an anechoic wind tunnel at École Centrale de Lyon [6, 9]. Some low-noise OGV concepts achieved noise reductions between 4 dB and 7 dB for both tonal and broadband noise. Secondly, the two most promising OGV concepts were adapted for a realistic experiment in the ECL5 fan-OGV stage. The reference configuration of the fan stage was then designed, fabricated and characterized in the framework of the Cleansky 2 Project CATANA [3].

This paper focuses on the experimental aero-acoustic characterization of innovative serrated and slitted OGVs to achieve a significant noise reduction in a 20” fan stage. This paper is organized as follows. Section II presents the PHARE-2 anechoic test facility at École Centrale de Lyon, where the the aerodynamic and acoustic tests were performed. An overview of the slitted and serrated OGVs is also included here. Section III presents the main aeroacoustic results, including a discussion on the aerodynamic penalty of the leading edge features and on the noise reduction in both upstream and downstream directions. Finally, Section provides a summary of the main findings and perspectives.

II. Experimental set-up

A. The ECL-B3 PHARE-2 facility

The experimental test campaigns were performed at the PHARE-2 test-rig at École Centrale de Lyon in France. The facility consists of a highly instrumented ducted fan-OGV stage without core flow, installed in an anechoic chamber. The shaft is driven up to a maximum rotational speed of 16 000 rpm by an electrical engine, with a maximum shaft power of 3 MW. Details on the facility are given in Ref. [20] and [3]. Upstream of the facility, the air flow passes through acoustic baffles on the roof of the building. Foam wedges are installed on the walls of the anechoic chamber to ensure low background noise and high-quality acoustic measurements [20]. Additionally, a turbulence control screen (TCS) is installed at the fan intake to ensure homogeneous inflow conditions and to reduce large-scale turbulence. The machine is instrumented with rakes and a Venturi nozzle for performance measurements. The rakes are removed for acoustic measurements to avoid spurious noise sources. During the experiments, the machine was stabilized at a constant rotational speed, corrected to ISA conditions. The operation point varied through incremental closing of an axisymmetric throttle downstream of the fan-OGV stage. Further details on the aerodynamic instrumentation and experimental methods can be found in Ref. [21] and [10].

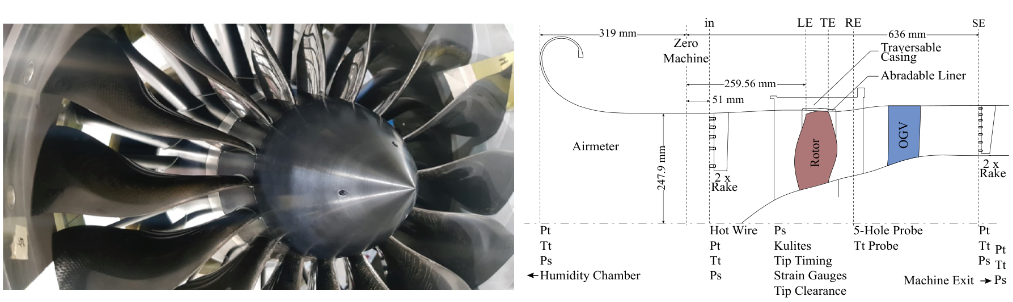

a) Fan Assembly ECL5 (CATANA) b) Schematic of Test Facility Core

Fig. 1 ECL5 open-test-case fan and machine.

As shown in Fig. 2, a total of 187 microphones are used in the test-rig to provide extensive data of the noise radiation from the fan-OGV stage. These microphones are distributed as follows. A total of 27 G.R.A.S. 46BE-S4 1/4" free-field microphones are mounted upstream of the fan intake on a 2m radius arch that can be rotated around the vertical axis. This is useful to measure the directivity over a portion of a sphere. Additionally, 160 flush-mounted G.R.A.S. 46BG 1/4" microphones are randomly-distributed in the duct and can be used to extract the modal amplitudes of the wall pressure fluctuations. Some of the in-duct microphones are mounted on rotating rigs. The current experimental set-up was used in previous studies to characterize fan stages for industrial UHBR turbofan engines, including acoustic measurements [20], modal decomposition methodologies [15], and aerodynamic instabilities [4].

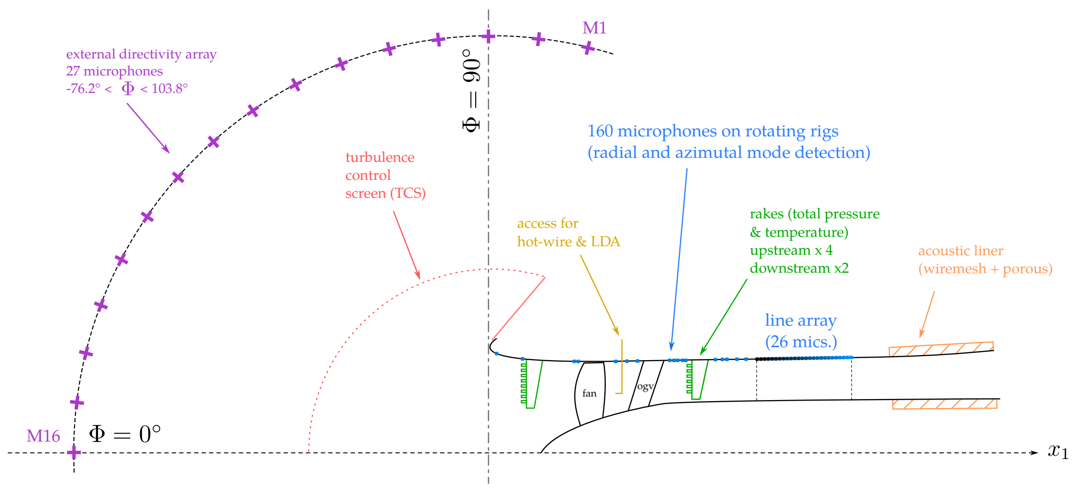

Fig. 2 Cross-section of the fan rig with the main instrumentation for multi-disciplinary analysis.

In the present work, the low-noise OGV concepts are tested in the ECL5/CATANA fan stage, which is an UHBR open test-case. This fan stage is a 1:4 scale rig and is representative of a modern UHBR fan designed and tested at the PHARE-2 facility at École Centrale de Lyon [3, 4, 13, 19]. The fan stage is shown in Fig. 1. It comprises 16 composite fan blades and 31 stator blades manufactured in aluminium. The aerodynamic design point was numerically predicted at a standard mass-flow rate of 36.0 kg/s, with a total pressure ratio of approximately 1.35 and an isentropic efficiency of about 92%.

B. Design of the leading edge features using slits and serrations

In this paper, two different types of leading edge features are investigated for the low-noise OGVs. The first OGV concept presents a slitted leading edge, whereas the second OGV concept presents leading edge serrations (see Fig. 3). Both innovative OGV designs have been optimized to reduce interaction noise based on local values of turbulence intensity and length scale in the fan wakes. These are useful to determine the optimal wavelength and amplitude of the leading edge features. Furthermore, the sweep angle of the baseline OGV is relatively small, which is convenient to assess the effectiveness of the leading edge features.

The design of the leading edge serrations is based on a previous work to determine the optimal wavelength and amplitude for providing maximum noise reductions [17]. Further details on the leading edge serrations that are presented in this paper are available in Ref. [7].

III. Experimental results and discussion

A. Aerodynamic performance of the fan-OGV stage

The iso-speed lines of the fan stage at 55%, 80% and 100% of the nominal rotational speed are indicated in Figure 4. For brevity, the detailed analysis of the aerodynamic performance and noise reduction of each OGV concept focuses on three different operating points A, B and C, which are shown in Figure 4. Points A (55%) and B (80%) were chosen at reduced rotational speeds on the same operating line as the design point C. It should be noted that 55% and 80% of the nominal rotational speed are representative of the fan speed at approach and take-off conditions. Point C at 100% of the nominal rotational speed corresponds to the design point of the fan stage.

Values of the pressure ratio and of the mass-flow rate are indicated in Table 1 for the baseline case and for the two low-noise OGV concepts. In table 1, the values of isentropic efficiency of the fan-OGV stage are also indicated. The aerodynamic penalties of the two low-noise concepts are included as well. Figure 4 shows that both modified OGV configurations present a slightly reduced stage pressure ratio than the baseline. The shape of the characteristics differs

Fig. 3 Low-noise OGVs with leading edge features. Slitted OGV mounted on the test-rig without the fan blades (left) and serrated OGV compared to the baseline OGV with straight leading edge (right).

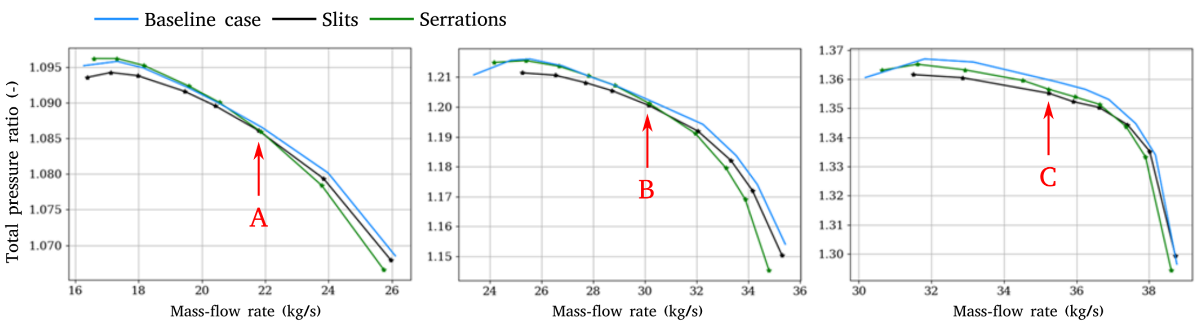

Fig. 4 Fan stage characteristics at 55% (left), 80% (center) and 100% (right) of the nominal rotational speed.

between slits and serrations. At low mass flow rates, the slits lead to a significantly decreased stage pressure ratio, while serrations are closer to baseline. shape In contrast, serrations show higher total pressure losses at near choke conditions.

OGV configuration	Mass-flow rate (kg/s)	Total pressure ratio	Isentropic efficiency (%)	Aerodynamic penalty (pts)
Baseline 55% (A)	21.9	1.087	92	-
Slits 55%	21.8	1.086	90.7	1.3
Serrations 55%	21.9	1.086	90.1	1.9
Baseline 80% (B)	30.2	1.202	92.6	-
Slits 80%	30.1	1.200	91.6	1.0
Serrations 80%	30.2	1.201	91.7	0.9
Baseline 100% (C)	35.5	1.360	92.3	-
Slits 100%	35.2	1.355	91.2	1.1
Serrations 100%	35.3	1.357	91.9	0.4

Table 1 Values of mass-flow rate, total pressure ratio and isentropic efficiency of the fan stage for the tested configurations. The aerodyamic penalties are defined as the difference between the isentropic efficiency of the baseline configuration and the low-noise OGV concepts.

At operating point A (see Figure 4 on the left), the isentropic efficiency of the baseline fan stage is 92%. Compared to the baseline case, the aerodynamic penalty at this operating point is about 1.3 pt for the slits, and 1.9 pt for the serrations. Other operating points at 55%, which have not been included in the present paper, show aerodynamic penalties below 1 pt for mass flow rates below 20 kg/s. For example, the minimum aerodynamic penalty for the OGV slits at 55% of the nominal rotational speed is about 0.7 pt at 20 kg/s. This suggests that the aerodynamic penalty of a low-noise OGV depends on the location along the iso-speed line of the fan, and therefore the OGV design could be optimized to minimize the impact at operating points near cruise condition.

At operating point B (see Figure 4 in the middle), the isotropic efficiency of the fan stage is around 92.6%. The slitted OGV presents an aerodynamic penalty of approximately 1 pt, which corresponds to the minimum penalty for this concept at about 30 kg/s, whereas the serrated OGV leads to slightly lower penalties of about 0.9 pt. For other operating points at 80% of the nominal rotational speed, which are not included in the present paper, aerodynamic penalty is below 0.5 pt for some operating points along the iso-speed line of the serrated OGVs.

At operating point C (see Figure 4 on the right), which corresponds to the design point at the nominal rotational speed of the fan stage, the slitted OGV leads to a 1.1 pt penalty compared to the baseline case, whereas it is around 0.4 pt for the serrated OGV. For different mass-flow rates up to approximately 37 kg/s, which are not shown in the present paper, the serrated OGV shows an excellent aerodynamic behavior with less than 0.5 pt penalties along the iso-speed line at 100% of the nominal rotational speed.

Overall, both low-noise OGV concepts show an isentropic efficiency penalty that can vary between 0.4 pt and 1.9 pt depending on the iso-speed lines and the operating point. The efficiency penalty is lower for the serrated OGV at high rotational speeds whereas it is lower for the slitted OGV at part-speed.

The total pressure contours were obtained using pressure rakes over an angular sector of 12° downstream of the OGV, which is sufficient to analyze a vane passage between two consecutive stator vanes. Each rake contains 7 total pressure probes, details provided in [21]. The total pressure contours are shown in figure 5 at the nominal rotational speed (point C from figure 4 on the right) for the baseline and the two low-noise OGV concepts. In this figure, the total pressure deficit in white color is caused by the OGV wakes, whereas the dark red area corresponds to the air flow in the OGV passage between adjacent vanes. The OGV wake width can be estimated from these measurements. At the mid-span probe, which is located at the radial location $R = 215$ mm, the wake width is approximately 12 mm for both baseline and serrated OGVs. However, the slitted OGV presents an increased wake width of approximately 17 mm. This is consistent with the results in Table 1, which show higher aerodynamic losses for the slitted OGVs when compared with the serrated OGVs.

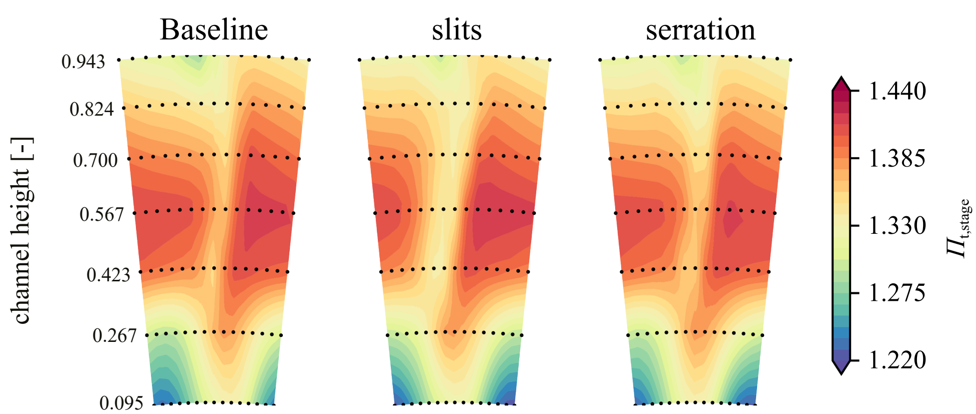

Fig. 5 Total pressure contours downstream of the OGVs over an angular sector of 12° for the baseline OGV (left), slitted OGV (middle) and serrations OGV (right) at operating point C.

B. Noise reduction using innovative OGV concepts

1. Free-field and in-duct noise spectra

Noise spectra are computed from acoustic measurements collected over 60 s with a sampling frequency of 102.4 kHz. The narrow-band spectra are estimated using the Welch method, with rectangular windows, blocs of 250 ms and a 50% overlap, which leads to a frequency resolution of 4 Hz. In the following sections, the spectra are presented as a function of the engine order (EO), defined as the ratio between the frequency and the rotational frequency of the shaft. The blade passing frequency (BPF) is also used, defined as the engine order multiplied by the number of fan blades.

Narrow-band spectra in the upstream direction are first presented in Fig. 6, for operating points A, B and C (see Fig. 4). These spectra were measured at 83° with respect to the fan axis at microphone location M4 (see Fig. 2). Upstream of the fan intake, the noise spectra from the fan-OGV stage exhibit two main acoustic contributions. Fistly, there is a tonal noise contribution at the BPF harmonics, which corresponds to engine orders 16, 32, etc. This tonal contribution is mainly generated by the periodic interaction of the mean flow deficit in the fan wakes with the OGV leading edge. Secondly, there is a broadband noise contribution, due to the turbulence in the fan wakes and in the boundary layers. At 100% of the nominal rotational speed (point C), the fan tip becomes transsonic and some additional tones may appear at the engine orders (EO), which indicates the onset of buzz saw noise.

At operating points A and B, the slitted OGV (in black) exhibits a broadband noise reduction that can vary between 2 dB and 4 dB compared to the baseline OGV (in blue). The serrated OGVs exhibit a larger noise reduction above the 3rd BPF approximately. For example, a broadband noise reduction of about 3 to 5 dB can be achieved depending on the rotational speed and target frequency range. The maximum noise reduction with both innovative OGV concepts is obtained between the 2nd and 5th harmonics of the BPF, i.e. between 3 and 8 kHz approximately. This result highlights the effectiveness of the OGVs with leading edge features to reduce broadband interaction noise, which is expected to be dominant in this frequency range.

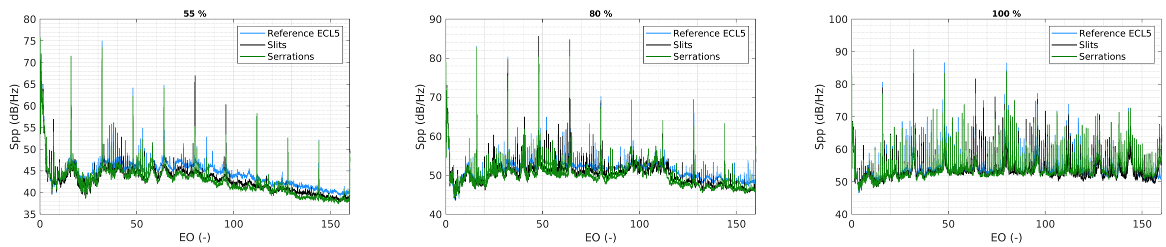

Fig. 6 Free-field noise spectra in the upstream direction at 2 m from the fan intake and 83° with respect to the fan axis for the three operating points A, B and C from Figure 4.

Tonal noise between the 1st (EO=16) and 4th (EO=64) harmonics of the BPF is shown in Fig. 13 at the same observer location as in Fig. 6. For the baseline OGV, it can be observed that the 2nd BPF is louder than the 1st BPF. This can be explained from Tyler & Sofrin's rule [22], which is based on the blade/vane count and cut-off circumferential modes in the duct. For the slitted OGVs, a significant tonal noise reduction of up to 10 dB approximately can be seen at the peak value for the 2nd and 4th BPFs at 55% of the nominal rotational speed (point A). However, the serrated OGVs exhibit an attenuation of about 1 dB or below between the 1st and 4th BPFs. At 80% of the nominal rotational speed (point B), the slitted and serrated OGV exhibit different behaviors for the tones in the upstream direction. For example, the serrated OGVs show a tonal noise reduction of about 5 dB at the 2nd BPF, 3 dB at the 3rd BPF, and 2 dB at the 4th BPF, whereas the slitted OGVs exhibit a tonal noise increase of 3 dB and 2 dB for the 3rd and 4th BPFs, respectively. These results indicates that the leading edge features of the OGVs can also be useful to reduce tonal interaction noise. Nevertheless, there might be a slight noise increase for some tones and observer angles. The upstream noise directivity and acoustic power will be useful to further investigate the effects of leading edge features on tonal noise.

In-duct acoustic measurements performed at approximately one chord length downstream of the OGVs are presented in Fig. 7 for the three operating points A, B and C. Unlike noise spectra from Fig. 6, which were measured in free-field, noise spectra from Fig. 7 were obtained from flush-mounted microphones in the duct. Wall-pressure spectra contain different contributions, including acoustic pressure fluctuations from the fan-OGV stage and turbulent pressure fluctuations from the boundary layers and fan/OGV wakes. At all three operating points A, B and C, both low-noise OGV concepts lead to a reduction in broadband noise of approximately 3 dB. However, this noise reduction is partly attributed to a reduction in the downstream propagating noise from the fan-OGV stage. An accurate estimation of the broadband noise reduction in the downstream direction is proposed in Section III.B.4 using a modal decomposition technique, which enables the separation of acoustic and turbulent pressure fluctuations.

At operating point A (55% of the nominal rotational speed), an increase in tonal noise of up to 8 dB in the peak value can be observed for both OGV concepts, except for the 1st BPF which presents a tonal noise reduction of 3 dB for serrated OGVs and of 5 dB for the slitted OGVs (see Fig. 14). At operating point B (80% of the nominal rotational speed), the innovative OGV concepts seem to slightly increase the 1st BPF obtained, whereas the amplitude of higher

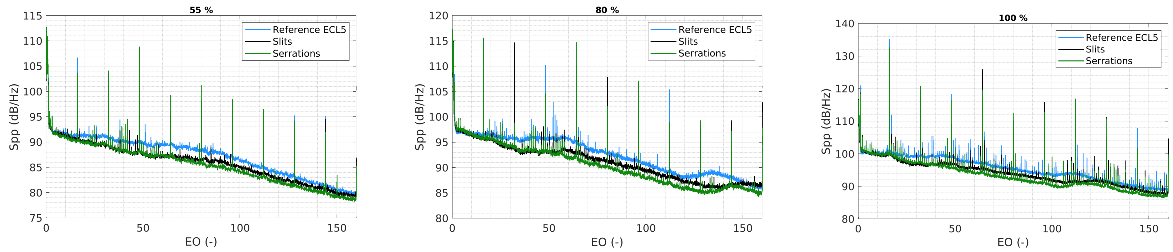

Fig. 7 In-duct acoustic spectra at one chord length downstream of the OGV trailing edge for the three operating point A, B and C from Figure 4.

order harmonics tends to decrease. At the nominal rotational speed (point C, see Figure 4 on the right), a different behavior is observed for tonal noise. Both OGV concepts can reduce tonal noise successfully at all BPF harmonics. For the slitted OGV, a significant tonal noise reduction of more than 10 dB can be observed for tones below the 3rd BPF. The tonal noise reduction in the downstream direction is less pronounced for the serrated OGV, in which the amplitude of the tones below the 3rd BPF is reduced by approximately 2 to 3 dB. It should be noted that the tonal noise reduction may slightly vary for neighboring in-duct microphones, although the trends are expected to be similar.

2. Upstream noise directivity

Microphone signals were recorded for a total of 33 angular positions of the external directivity array (see Fig. 2), such that it is possible to represent the three-dimensional directivity over a semi-sphere. In this section, the noise spectra from the external directivity array are integrated for frequencies above 2 kHz, as shown in Fig. 8. High levels of broadband noise can be observed between approximately 30° and 70°, with respect to the fan axis. The insertion loss (IL), which is defined here as the difference in dB between the baseline OGV and a low-noise OGV concept, is represented in Figure 9.

Both serrated and slitted OGVs present a significant broadband noise reduction for most observer angles in the upstream direction. The maximum acoustic benefit can be found at off-axis observers, where a broadband noise reduction of 2 to 5 dB can be observed for most observer angles at all operating points. The broadband noise reduction seems to be slightly smaller at the design point for the nominal rotational speed (point C). This might be explained by an increase of the tonal contribution because of buzz-saw noise, together with a reduction in the fan wake turbulence which reduces broadband interaction noise at the design point. Nevertheless, both the slitted and serrated OGV designs seem to be quite robust, as both OGV concepts can provide a significant acoustic benefit for different operating points of the fan. Finally, it can be observed a small noise reduction or increase of about 2 dB for observer angles close to the fan axis when using innovative OGV concepts, depending on the operating point and the leading edge features. Nevertheless, the contribution of the noise radiated close to the fan axis is expected to have little effect on the upstream acoustic power.

3. Upstream sound power level

The sound power level (PWL) is computed from the external directivity array (see Fig. 2), aligned with the fan axis. In the following, noise radiation is assumed to be axisymmetric, since the fan intake is axisymmetric, and since the fan-OGV configuration is homogeneous, i.e. in the absence of struts or heterogeneous OGVs. The upstream PWL is shown in Fig. 10. Noise reductions between 3 to 5 dB are observed for both slitted and serrated OGVs, which is consistent with previous findings at a discrete observer angle (for example, see microphone M4 at 83° with respect to the fan axis in Fig. 6).

4. Downstream modal decomposition

Advanced instrumentation of the ECL-B3 test-bench also allows the noise to be measured downstream of the rotor-stator stage. Downstream of the OGVs, wall-pressure fluctuations are measured by a large set of wall flush-mounted microphones. An example of narrow-band spectrum, measured approximately 2 OGV chords downstream of the stators trailing edges, is indicated in Fig. 7. Compared to the baseline ECL5 - CATANA configuration, the low-noise OGV INNOSTAT concept exhibits a broadband noise reduction of 2 to 3 dB, depending on the frequency. However, using flush-mounted microphones, an additional contribution to pressure fluctuations is added because of wall-bounded

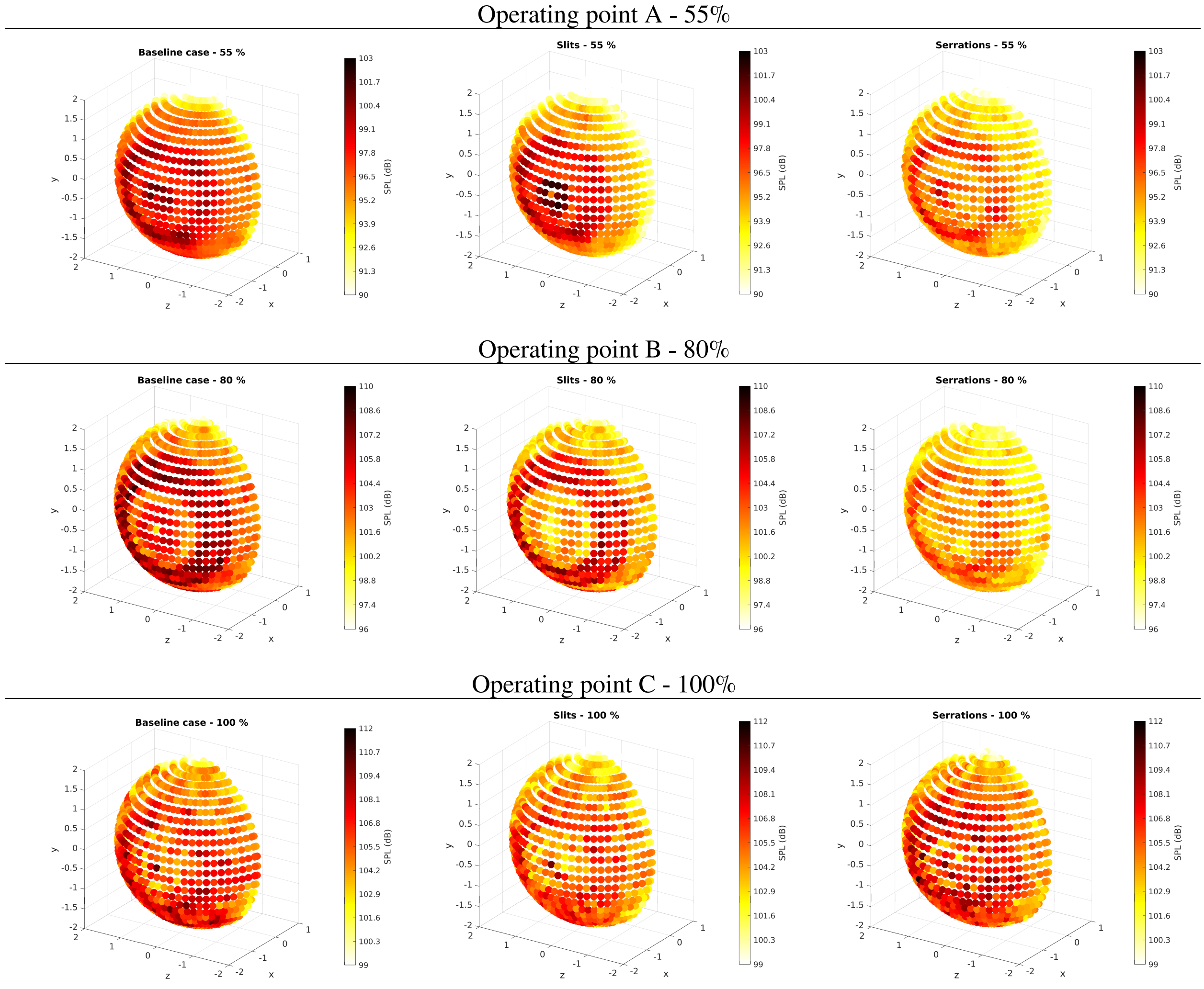

Fig. 8 Three-dimensional directivity of broadband noise, integrated for frequencies above 2 kHz, at 2 m from the fan intake. On the left, baseline OGV. In the middle, slitted OGV. On the right, serrated OGV.

turbulence, which can be higher than the pure acoustic pressure fluctuations. The modal analysis presented in the following is able to separate both components and to offer a non-ambiguous estimation of the insertion loss of the innovative OGV concept. Note that, for the tonal components visible on the narrow-band spectra, since the signals are largely dominated by the acoustic contribution, it is possible to directly assess the noise reduction associated with the different OGV configurations. For example, at operating point B for the 4th BPF on Fig. 14 at right, a 13 dB noise reduction can be observed on the peak for the slitted OGVs. Nonetheless, the removal of the turbulent component of the signals remains interesting for the broadband noise analysis.

In the following, a broadband modal decomposition is performed over the flush-mounted microphones installed downstream of the rotor-stator stage. First, the tonal acoustic contribution of the fan stage was obtained through a phase-averaging of the microphone pressure signals. By subtracting this contribution to the pressure signals, a broadband signal is then obtained, which is used as input data for the modal decomposition. A detailed description of this post-processing technique is given in Ref. [15]. The modal amplitudes of downstream propagating waves are indicated in Fig. 11 for the three OGV configurations (baseline, slits and serrations) at the three different operating conditions. In these figures, m is the azimuth mode order, and the contributions of all cut-on radial orders for fixed m have been integrated.

All cases show dominant mode amplitudes close to cut-on/cut-off boundaries for both co- and counter-rotating

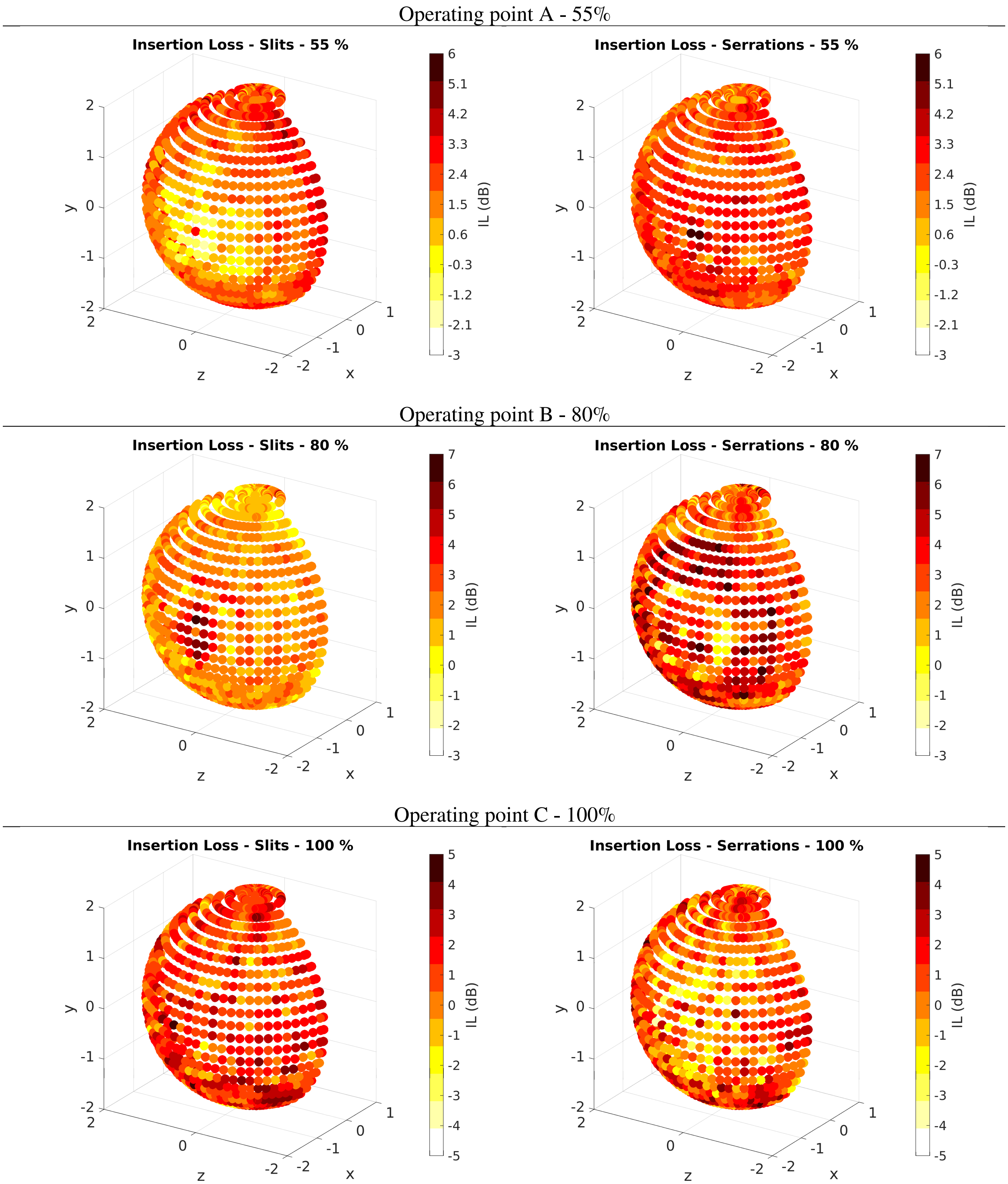

Fig. 9 Insertion loss (IL) of the low-noise OGV concepts. IL > 0 dB corresponds to a noise reduction, which is indicated by orange and red colors.

modes. Apart from these spots originating from the modes frequency cutoff, the baseline OGV configuration shows high mode amplitudes for counter-rotating modes of high azimuth orders, $-10 < m < -5$. This can be explained by an equivalent dipole reasoning. The contribution of stator leading edge noise tends to favour counter-rotating modes

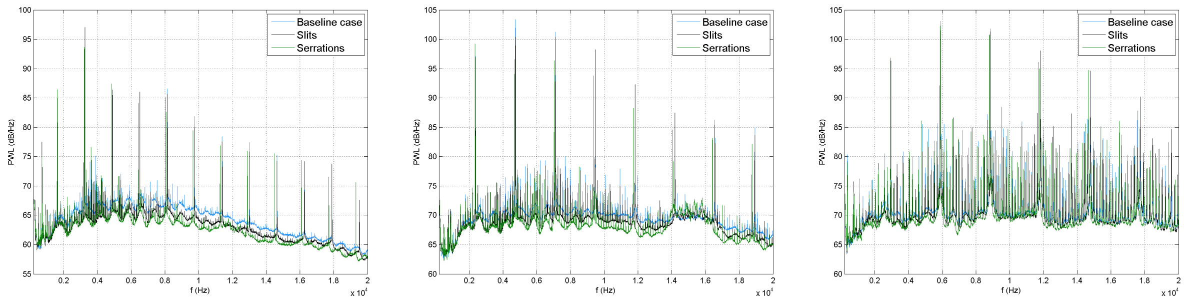

(a) 55% **(b) 80%** **(c) 100%**

Fig. 10 Upstream sound power level computed from the external directivity array.

downstream of the stator, see Ref. [16]. This contribution is located around the frequency band from 4 to 8 kHz at 55% of the nominal rotational speed, from 4 to 7 kHz at 80%, and from 3 to 6 kHz at 100% approximately, see first row of Fig. 11.

This contribution is well attenuated by the slits concept, by a factor between 5 to 10 dB depending on the operating conditions. The serrations concept is less efficient for this contribution ; a maximum noise reduction of around 5 dB is observed, depending on the operating conditions. Additionally, high mode amplitudes close to the frequency cut-off of high order modes are also attenuated by the two concepts, with a noise reduction on the order of 2 to 3 dB. On the contrary, low orders modes with $|m| < 5$ are not or very little attenuated, which is consistent with the directivity maps of Fig. 8 where the efficiency of the low-noise OGV concept is quasi null in the test-rig axis, especially for the slits concept.

The complete modal breakdown gives estimates of both azimuth and radial mode amplitudes $A^+_{m,n}$. The individual mode sound power $W^+_{m,n}$ is then easily obtained. Finally the total duct sound power transmitted downstream W^+ can be obtained by integrating over all azimuth and radial mode orders. This procedure is carried out for the baseline case and the two low-noise configurations. The result is indicated in Fig. 12 as power spectra. The insertion loss, defined as the ratio in decibels between the two cases, is indicated in the second row of Fig. 12.

Downstream of the rotor-stator stage, a maximum insertion loss of 10 dB is obtained with the slits at engine order 57 around 6 kHz, at 55% of the nominal rotational speed. With the serrations, the efficiency of the low-noise concept grows with the frequency to reach values over 10 dB at high frequencies. This finding suggests a potential overestimation of noise reduction predictions for this concept. Indeed, at high frequencies, the modal decomposition approach may be influenced by a low signal-to-noise ratio. Further investigation is ongoing to conclusively determine the validity of these results. At higher rotational speeds, similar conclusions can be drawn, except that the efficiency is a bit lower, with maximum insertions losses around 8 dB.

IV. Conclusion

In this paper, findings of the collaborative INNOSTAT research project, involving different institutions and private companies in Europe, are reported. Two different low-noise OGV concepts, previously tested in a linear wind tunnel cascade, were analyzed in the present paper. The first concept uses slits on the leading edges of the stator vanes, and the second concept uses serrations. Both concepts wavelength and geometrical parameters were specifically designed to account for the specific aerodynamic conditions encountered on the transsonic ECL5 - CATANA open fan test-case, which serves as the baseline case of the study. Microphone measurements at the design point of the stage and at lower rotational speeds were analyzed upstream of the duct to extract the external upstream radiated noise. Also, in-duct wall-pressure measurement downstream of the rotor-stator stage could be processed to obtain the modal amplitudes of the three configurations (baseline case, slits and serrations).

At 55% of the nominal rotational speed, upstream radiated noise could be reduced up to 6 dB, depending on the frequency. Tonal components, such as the harmonics of the blade passing frequency, could be attenuated up to 10 dB approximately. The maximum efficiency is obtained off-axis. In the test-rig axis, very little attenuation is observed, or even a slight increase of the radiated noise around 1 dB. Downstream of the stage, the modal decomposition performed on both configurations enabled a fine observation of the modal content modifications due to the leading edge features of the OGV. At the design point of the fan, we observed an attenuation of both co- and contra-rotative modes amplitudes up

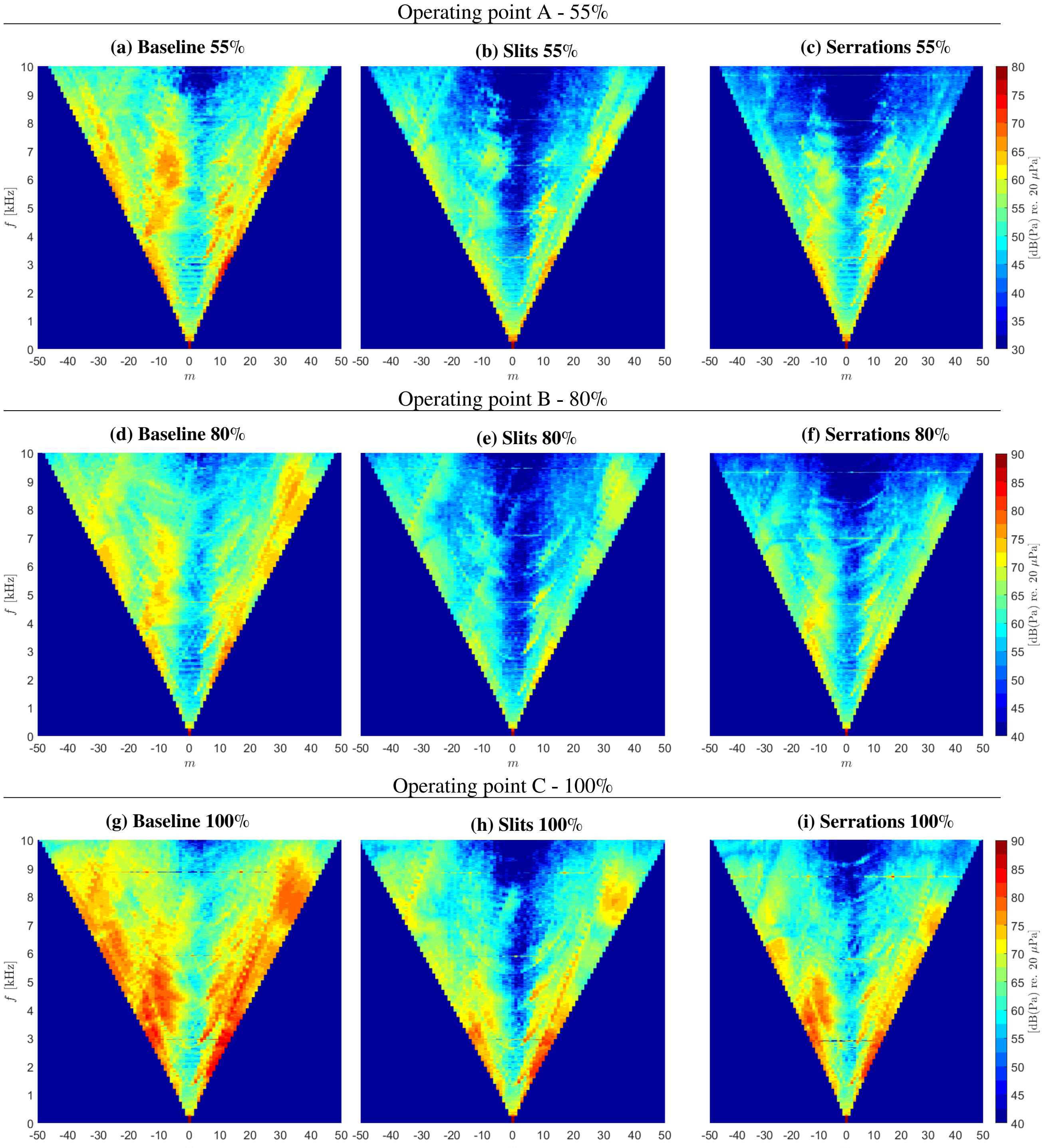

Fig. 11 Broadband modal content downstream of the rotor-stator stage for the three tested OGV geometries and for different operating conditions at the design point working line. The frequency is plotted against the azimuth mode order and the mode amplitudes A_m^+ are colored by their amplitude.

to 8 dB approximately. The OGV concept is less effective for low-order modes below 5. The total acoustic power could be obtained by integrating over the cut-on modes of the duct, and the efficiency of the concept, estimated downstream of the stage for broadband noise, is above 5 dB with a maximum of 10 dB. Locally, the efficiency can be found over 13 dB

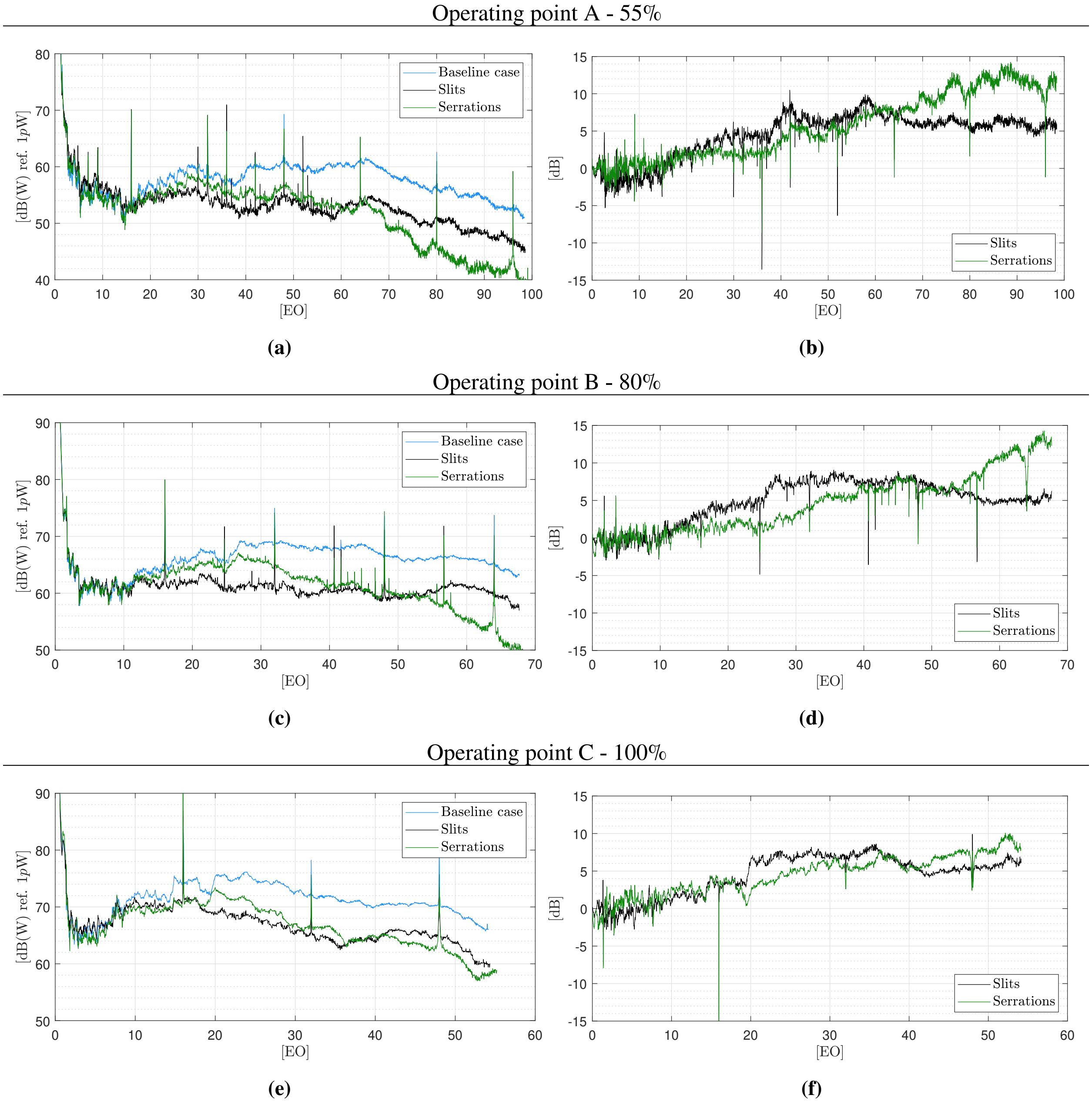

Fig. 12 Estimates of the in-duct sound power transmitted downstream of the rotor-stator stage for the three tested configurations at (a) approach 55%, (c) cutback 80% and (e) 100%. Ratio between the sound power of baseline and innovative concepts for three operating conditions: (b) approach 55%, (d) cutback 80% and (f) 100 %.

for tonal components.

Acknowledgments

The authors are particularly grateful to Benoit Paoletti and Cédric Desbois for their help in setting up and conducting the experiments in the PHARE-2 facility. This research was performed within the framework of the Labex CeLyA of the Université de Lyon (program "Investissements d'Avenir" ANR-10-LABX-0060/ANR-11-IDEX-0007), operated by the ANR. This study has received funding from the CleanSky 2 Joint Undertaking (JU) under the European Union

Horizon 2020 research and innovation program, grant agreement n°865007 INNOSTAT project. The authors are also grateful to Safran Aircraft Engines for the additional funding and for the continuous support since the beginning of the PHARE-2 project.

Tonal noise reduction at the BPF harmonics

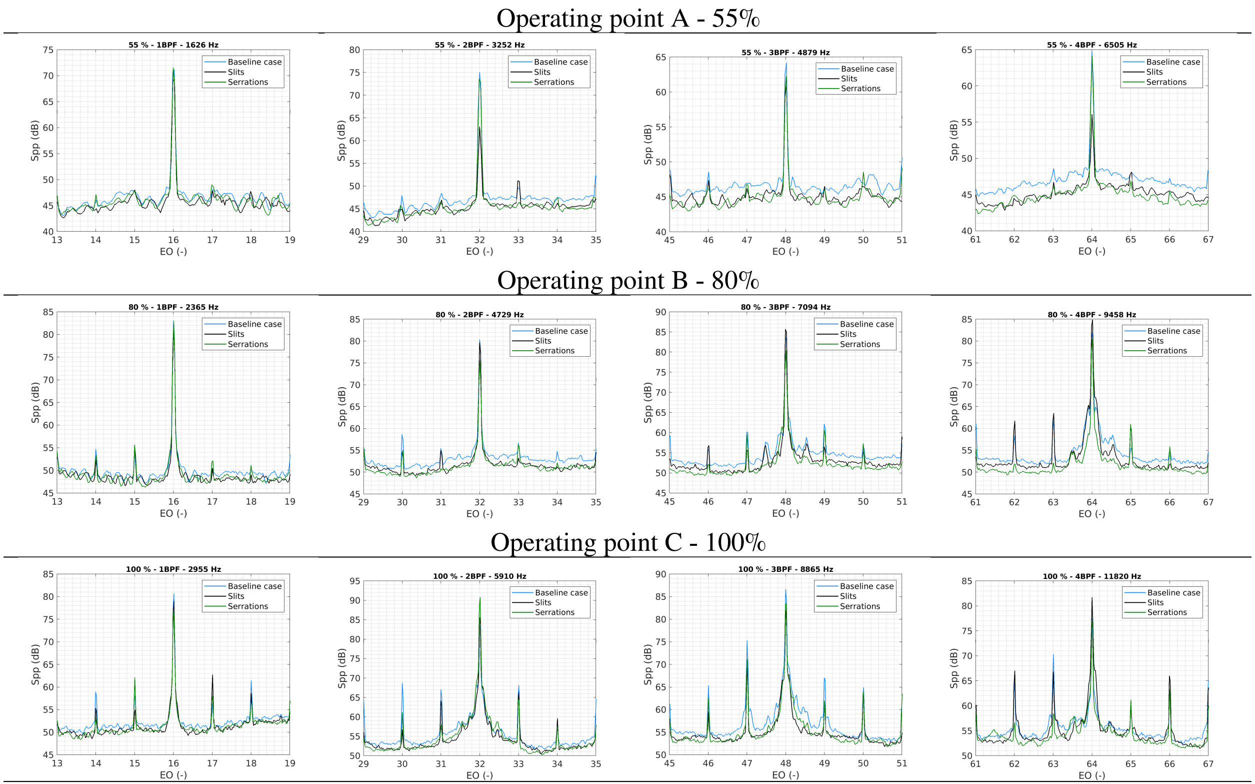

Fig. 13 Free-field noise spectra around BPFs 1 to 4 in the upstream direction at 2 m from the fan intake and 83° with respect to the fan axis for the three operating points A, B and C (see also Figure 6).

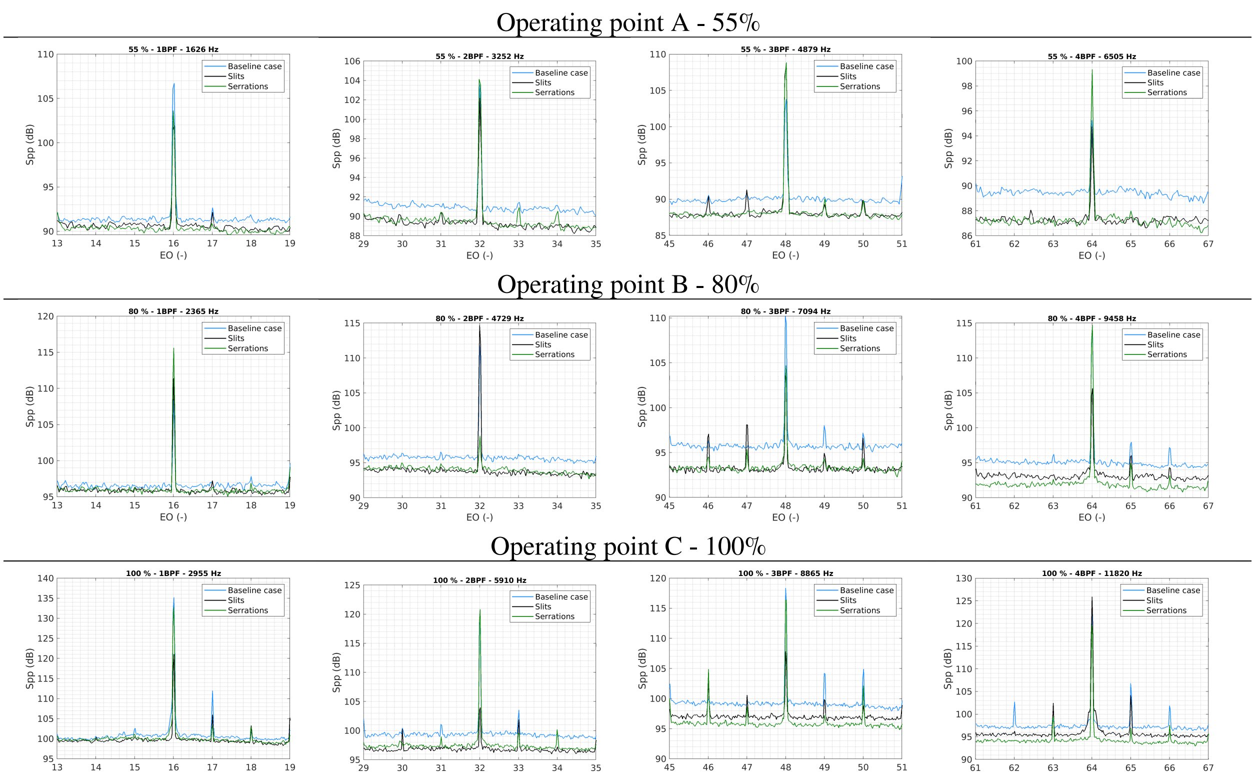

Fig. 14 In-duct acoustic spectra around BPFs 1 to 4 at one chord length downstream of the OGV trailing edge for the three operating point A, B and C (see also Figure 7).

References

[1] L. Ayton and C. Paruchuri, "An analytical and experimental investigation of aerofoil–turbulence interaction noise for plates with spanwise-varying leading edges",*J. of Fluid Mec.*, **865**, pp 137–168, 2019. https://doi.org/10.1017/jfm.2019.78

[2] K. Billon, E. De Bono, M. Perez, E. Salze, G. Matten, M. Gillet, M. Ouisse, M. Volery, H. Lissek, J. Mardjono, M. Collet, "In flow acoustic characterisation of a 2D active liner with local and non local strategies", *Applied Acoustics*, **191**:108655, 2022. https://doi.org/10.1016/j.apacoust.2022.108655

[3] C. Brandstetter, V. Pages, P. Duquesne, B. Paoletti, S. Aubert, X. Ottavy, "Project PHARE-2— a high-speed UHBR fan test facility for a new open-test case.", *J. Turbomach.*, **141**(10): 101004, 2019. https://doi.org/10.1115/1.4043883

[4] C. Brandstetter, B. Paoletti, X. Ottavy, "Compressible Modal Instability Onset in an Aerodynamically Mistuned Transonic Fan", *ASME. J. Turbomach*, **141**(3):031004, 2019. https://doi.org/10.1115/1.4042310

[5] M. Buszyk, C. Polacsek, T. Le Garrec, R. Barrier and C. Bailly, "Numerical assessment of turbulence-cascade noise reduction and aerodynamic penalties from serrations, *AIAA J.*, **60**(6), 2022. https://doi.org/10.2514/1.J061301

[6] M. Buszyk, C. Polacsek, T. Le Garrec, R. Barrier, V. Clair, E. Salze, and C. Bailly, "Aeroacoustic assessment of a rectilinear cascade with leading edge serrations: Predictions and measurements", submitted to *Computers* & *Fluids* (accepted), 2023.

[7] M. Buszyk, C. Polacsek, T. Le Garrec, R. Barrier, E. Salze and J. Mardjono, "Aeroacoustic performances of ECL5 UHBR turbofan model with serrated OGVs: design, predictions and comparisons with measurements", AIAA 2024-3168. 30th AIAA/CEAS Aeroacoustics Conference, 2024.

[8] D. Casalino, F. Avallone, I. Gonzalez-Martino, and D. Ragni, "Aeroacoustic study of a wavy stator leading edge in a realistic fan/OGV stage", *J. of Sound and Vib.*, **442**, pp138–154, 2019. https://doi.org/10.1016/j.jsv.2018.10.057

[9] V. Clair, É. Salze, P. Souchotte and E. Jondeau. "Turbulence interaction noise from a rectilinear cascade of airfoils and effects of porous material inclusions," *AIAA 2023-4188*. AIAA AVIATION Forum, 2023. https://doi.org/10.2514/6.2023-4188

[10] A.-L. Fiquet, A. Schneider, B. Paoletti, X. Ottavy and C. Brandstetter,"Experiments on tuned UHBR open-test-case fan ECL5/CATANA: stability limit", Proc. ASME Turbo Expo 2023, GT2023-102537. https://hal.science/hal-04066078v1

[11] INNOSTAT H2020 Cleansky 2 European Project public website, https://www.innostat-cs2.eu/

[12] M. Munjal, *Acoustics of ducts and mufflers with application to exhaust and ventilation system design*, Wiley-Interscience publication, Wiley, 1987.

[13] V. Pagès, P. Duquesne, S. Aubert, L. Blanc, P. Ferrand, X. Ottavy, C. Brandstetter, "UHBR Open-Test-Case Fan ECL5/CATANA", *Int. J. of Turbomachinery, Propulsion and Power*, **7**(2):17, 2022. https://doi.org/10.3390/ijtpp7020017

[14] C. Paruchuri, P. Joseph, S. Narayanan, C. Vanderwel, J. Turner, J.W. Kim and B. Ganapathisubramani, "Performance and mechanism of sinusoidal leading edge serrations for the reduction of turbulence–aerofoil interaction noise", *J. of Fluid Mec.*, **818**, 2017. https://doi.org/10.1017/jfm.2017.141

[15] A. Pereira, E. Salze, J. Regnard, F. Gea-Aguilera, M. Gruber, "New modular fan rig for advanced aeroacoustic tests - Modal decomposition on a 20" UHBR fan stage", AIAA 2019-2604. 25th AIAA/CEAS Aeroacoustics Conference, 2019. https://doi.org/10.2514/6.2019-2604

[16] Pereira, A. and Jacob, M.C., "Modal analysis of in-duct fan broadband noise via an iterative Bayesian inverse approach", *J. of Sound and Vib.*, **520**, pp116633, 2022. https://doi.org/10.1016/j.jsv.2021.116633

[17] C. Polacsek, A. Cader, M. Buszyk, R. Barrier, F. Gea-Aguilera and H. Posson, "Aeroacoustic design and broadband noise predictions of a fan stage with serrated outlet guide vanes, *Physics of fluids*, **32**(10), 2020. https://doi.org/10.1063/5.0020190

[18] E. Rivet, S. Karkar, H. Lissek, "Broadband low-frequency electroacoustic absorbers through hybrid sensor-/shunt-based impedance control", *IEEE T. Contr. Syst. T.* **25**(1), pp 63-72, 2016. https://doi.org/10.1109/TCST.2016.2547981

[19] M. Rodrigues, L. Soulat, B. Paoletti, X. Ottavy, C. Brandstetter, "Aerodynamic investigation of a composite low-speed fan for UHBR application", *J. Turbomach.* **143**(10):101004, 2021. https://doi.org/10.1115/1.4050671

[20] E. Salze, A. Pereira, P. Souchotte, J. Regnard, F. Gea-Aguilera, M. Gruber, "New modular fan rig for advanced aeroacoustic tests - Acoustic characterization of the facility", AIAA 2019-2603. 25th AIAA/CEAS Aeroacoustics Conference, 2019. https://doi.org/10.2514/6.2019-2603

[21] A. Schneider, A.-L. Fiquet, B. Paoletti, X. Ottavy and C. Brandstetter, "Experiments on tuned UHBR open-test-case fan ECL5/CATANA: performance and aerodynamics", Proc. ASME Turbo Expo 2023, GT2023-103629. https://hal.science/hal-04066082

[22] Tyler, J. M. and Sofrin, T. G., "Axial Flow Compressor Noise Studies", *SAE Technical Paper*, **620532**, 1962. http://dx.doi.org/10.4271/620532